

Radiation-induced Apoptosis of Endothelial Cells in the Murine Central Nervous System: Protection by Fibroblast Growth Factor and Sphingomyelinase Deficiency¹

Louis A. Peña, Zvi Fuks, and Richard N. Kolesnick²

Laboratory of Signal Transduction [L. A. P., R. N. K.] and Department of Radiation Oncology [L. A. P., Z. F.], Memorial Sloan-Kettering Cancer Center, New York, New York 10021

ABSTRACT

Injury to the central nervous system (CNS) by ionizing radiation may be a consequence of damage to the vascular endothelium. Recent studies showed that radiation-induced apoptosis of endothelial cells *in vitro* and in the lung *in vivo* is mediated by the lipid second messenger ceramide via activation of acid sphingomyelinase (ASM). This apoptotic response to radiation can be inhibited by basic fibroblast growth factor or by genetic mutation of ASM. In the CNS, single-dose radiation has been shown to result in a 15% loss of endothelial cells within 24 h, but whether or not this loss is associated with apoptosis remains unknown. In the present studies, dose- and time-dependent induction of apoptosis was observed in the C57BL/6 mouse CNS. Apoptosis was quantified by terminal deoxynucleotidyl transferase-mediated nick end labeling, and specific endothelial apoptosis was determined by histochemical double labeling with terminal deoxynucleotidyl transferase-mediated nick end labeling and *Lycopersicon esculentum* lectin. Beginning at 4 h after single-dose radiation, apoptosis was ongoing for 24 h and peaked at 12 h at an incidence of 0.7–1.4% of the total cells in spinal cord sections. Up to 20% of the apoptotic cells were endothelial. This effect was also seen in multiple regions of the brain (medulla, pons, and hippocampus). A significant reduction of radiation-induced apoptosis was observed after i.v. basic fibroblast growth factor treatment (0.45–4.5 $\mu\text{g}/\text{mouse}$). Identical results were noted in C3H/HeJ mice. Furthermore, irradiated ASM knockout mice displayed as much as a 70% reduction in endothelial apoptosis. This study demonstrates that ionizing radiation induces early endothelial cell apoptosis throughout the CNS. These data are consistent with recent evidence linking radiation-induced stress with ceramide and suggest approaches to modify the apoptotic response in control of radiation toxicity in the CNS.

INTRODUCTION

Considerable effort has been made over the years to quantify the tolerance of normal tissues to provide a baseline for therapeutic irradiation at maximum biologically effective doses (1, 2). Normal tissue injury by ionizing radiation differs depending on the target organ and cell types. Acute or early reactions primarily reflect the balance between the rates of cell killing by irradiation and regeneration by surviving stem cells, whereas late reactions occur when radiation depletes the tissue stem cell compartment, leading to tissue necrosis, fibrosis, and organ dysfunction.

In the CNS,³ there is a high degree of cellular heterogeneity, and both early and late injuries occur (3, 4). Whereas symptoms of acute

and subacute injury can be reversed to some extent with steroid medication, the late forms of CNS injury are irreversible. The TD_{5/5}–TD_{50/5} for single-dose exposure are 15–20 Gy and are similar for spinal cord myelopathy, brain white matter necrosis (leukoencephalopathy), and microvascular damage (1). The pathogenesis of myelin degeneration and leukoencephalopathy is not fully understood. Whereas one hypothesis suggests that oligodendrocyte injury mediates this response, it is also possible that microvascular damage is a primary culprit (5–7). Acute vascular changes within 24 h after irradiation include increased endothelial cell swelling, vascular permeability and edema, lymphocyte adhesion and infiltration, and apoptosis (1, 8). Late vascular effects occur weeks to months after irradiation and include capillary collapse, thickening of basement membranes, scarring and fibrosis, teleangiectasias, and a loss of clonogenic capacity (1, 8).

Despite the importance of radiation effects on the vascular endothelium in the CNS, there are little current *in vivo* data on endothelial cell death, and that which does exist is contradictory. A study of irradiated rodent brain showed that up to 15% of endothelial cells are lost within 24 h of irradiation (9), the time frame in which apoptosis is most likely to occur. However, another study failed to detect any endothelial cell apoptosis within the same time frame (10, 11). The present work was undertaken to determine whether endothelial apoptosis occurs after CNS irradiation in a rodent model and to determine the mechanism of this response.

Recent studies have demonstrated that microvascular endothelial apoptosis constitutes an early and critical element in radiation pneumonitis and in the LPS-induced septic shock syndrome (12, 13). The proapoptotic effects of radiation and of LPS were shown to be mediated via the ASM and the generation of ceramide (13, 14). Genetic mutations that inactivate ASM or treatment with i.v. injections of bFGF abrogated ceramide generation and apoptosis. The same mechanism of radiation-induced apoptosis via ceramide generation was also observed in endothelial cells *in vitro* (15), and the antiapoptotic action of bFGF (16–18) was shown to be mediated, at least in part, via activation of the α isoform of PKC (17). A similar interaction between radiation, ceramide, PKC, and apoptosis was reported in the SQ-20B squamous carcinoma cell line, in which radiation failed to elicit an apoptotic response unless PKC was blocked, leading to increased apoptosis and clonogenic cell death *in vitro* and *in vivo* (19, 20). Radiation-induced apoptosis in lymphoid cells is similarly associated with a balance between ceramide and PKC activity, although in this system, Bcl-2 also regulated ceramide- and radiation-induced apoptosis (21, 22). Similarly, a loss of neutral sphingomyelinase has been shown to confer radiation resistance in WEHI-231 and TF-1 lymphoid cells, in which a reduction in both clonogenic death and apoptotic death was associated with deficient ceramide production (19, 20, 23). Zundel and Giaccia (24) have shown that stress signals apoptosis via ceramide-induced down-regulation of phosphatidylinositol 3'-kinase and inhibition of the kinase Akt/PKB. Inhibition of

Received 7/27/99; accepted 11/15/99.

The costs of publication of this article were defrayed in part by the payment of page charges. This article must therefore be hereby marked *advertisement* in accordance with 18 U.S.C. Section 1734 solely to indicate this fact.

¹ Supported by NIH/National Cancer Institute Research Career Development Award K01-CA-76483 (to L. A. P.) and NIH Grants CA-52462 (to Z. F.) and CA-42385 (to R. N. K.).

² To whom requests for reprints should be addressed, at Laboratory of Signal Transduction, Memorial Sloan-Kettering Cancer Center, 1275 York Avenue, Box 254, New York, NY 10021. Phone: (212) 639-8573; Fax: (212) 639-2767; E-mail: r-kolesnick@ski.mskcc.org.

³ The abbreviations used are: CNS, central nervous system; ASM, acid sphingomyelinase; FGF, fibroblast growth factor; bFGF, basic FGF; TdT, terminal deoxynucleotidyl transferase; TUNEL, TdT-mediated nick end labeling; LPS, lipopolysaccharide; PKC, protein kinase C; KO, knockout; TBST, 50 mM Tris (pH 7.5), 150 mM NaCl, and 0.1%

Triton X-100; LEL, *Lycopersicon esculentum* lectin; RCA-1, *Ricinus communis* agglutinin 1; aFGF, acidic FGF; DAB, 3,3'-diaminobenzidine tetrachloride.

this pathway resulted in decreased phosphorylation of Bad, a death effector in the Bcl-2 family. Signaling via the kinase suppressor of Ras/mitogen-activated protein kinase pathway may also cause the inactivation of Akt/PKB and the dephosphorylation of Bad, although direct data on ionizing radiation as the apoptotic stimulus for this pathway are currently lacking (25). Hence, radiation-induced apoptotic signaling through ceramide appears to involve multiple, coordinated pathways, and the apoptotic outcome *in vitro* and *in vivo* depends on the balance between the activities of pro- and antiapoptotic signaling systems.

In this report, we examined *in vivo* the extent and kinetics of CNS endothelial cell responses to radiation in the mature CNS of mice. Dose- and time-dependent induction of apoptosis was observed in the endothelium of the brain and spinal cord. A significant reduction of this apoptotic response was observed after *i.v.* bFGF treatment or in ASM KO mice. These radioprotective effects are consistent with an emerging body of evidence linking radiation-induced stress responses in endothelium with ceramide and suggest new approaches to modify the apoptotic response in the control of radiation toxicity in the CNS.

MATERIALS AND METHODS

Animals. Male C57BL/6, C3H/HeJ, and 129/Sv mice were purchased from Taconic (Germantown, NY) and housed in the Sloan-Kettering animal facility until reaching a specific age for each experiment (16 weeks old, unless stated otherwise). A colony of transgenic mice harboring a KO of the ASM gene (ASM KO) was established at our animal facility, having originally been obtained from Dr. Edward Schuchman (Department of Genetics, Mount Sinai School of Medicine, New York, NY; Ref. 26). These mice have a 129/Sv \times C57BL/6 genetic background, therefore wild-type individuals of this cross were used as controls in experiments involving ASM KO mice. It should be noted that whereas ASM KO mice begin to exhibit Niemann-Pick disease-like symptoms at approximately 20 weeks of age, experiments in this study were carried out using ASM KO animals at 8 or 16 weeks of age.

Irradiation. Mice were lightly sedated with ketamine (0.1 mg/g), placed prone in a ^{137}Cs irradiator (Shepherd Mark-I, Model 68), and subjected to total body irradiation at a dose rate of 220 cGy/min. At various time points, animals were euthanized and perfusion fixed intracardially with fresh 4% paraformaldehyde in PBS. Brains and spinal cords were dissected and post-fixed overnight and then placed in an automated vacuum tissue processor for paraffin embedding over a 16-h period. In some experiments, mice were also given *i.v.* injections of recombinant bFGF or other cytokines (R&D Systems, Minneapolis, MN) in a vehicle of 0.1% gelatin under metaphane anesthesia into the retro-orbital plexus according to the following schedule: 5 min before irradiation; immediately after irradiation; and 1 h after the start of irradiation.

Apoptosis and Histochemical Analyses. Noncontiguous 8- μm sections were mounted on slides, rehydrated, and stained using the TUNEL method for detection of apoptosis *in situ*, as described previously (16, 27). Briefly, slides were incubated with 3% H_2O_2 in PBS for 5 min, rinsed, and then incubated in TdT buffer [140 mM cacodylate (pH 7.2), 30 mM Tris, and 1 mM CoCl_2] for 15 min at 22°C. TdT reaction mixture was added [0.2 unit/ μl TdT (Boehringer Mannheim Roche; Indianapolis, IN), 2 nM biotin-11-dUTP (Boehringer Mannheim Roche), 100 mM cacodylate (pH 7.0), 2.5 mM CoCl_2 , 0.1 mM DTT, and 0.05 mg/ml BSA] and incubated for 30 min at 37°C. After blocking with 2% BSA and an incubation with avidin-biotin peroxidase complexes (ABC kit; Vector Laboratories; Burlingame, CA), the TUNEL reaction was visualized by chromogenic staining with DAB (Sigma, St. Louis, MO). Slides were counterstained with hematoxylin.

For immunohistochemical double labeling, TUNEL-stained sections were transferred at room temperature to TBST buffer, followed by blocking in 2% fetal bovine serum in TBST, three washes with PBS, and an overnight incubation at 4°C with rhodamine-conjugated LEL (Sigma) at a concentration of 25 $\mu\text{g/ml}$ in PBS (28, 29). After two washes with TBST and one 1-h wash with water, coverslips were mounted with Permafluor (Shandon Lipshaw; Pittsburgh, PA). Two alternative endothelial markers were used: (a) biotinylated RCA-1 (Vector Laboratories) at 30 $\mu\text{g/ml}$ (30–33) followed by incubation with rhodamine-conjugated avidin (Vector Laboratories); or (b) antimouse

CD31 monoclonal antibody (PharMingen; San Diego, CA) at a 1:50 dilution in PBS (13, 34, 35) followed by biotinylated antihuman IgG (PharMingen) at a 1:100 dilution [anti-CD31 was preceded by an antigen unmasking step of 20 min at 37°C with pepsin (Sigma; 60,000 units/ml) in water]. Stained slides were viewed with a Zeiss Axiophot-2 under light and/or epifluorescence illumination with rhodamine filter sets.

Cell counts of TUNEL- and double-labeled TUNEL + LEL-stained cells were counted manually in a single-blind fashion. Brown-stained nuclei immediately at the edge of a tissue section were excluded from cell counts to minimize false positives. Significant differences were determined by one-tailed Student's *t* test. For simple counts of the total number of cells per spinal cord cross-section, digital photomicroscopy images were acquired with a SPOT-32 charge-coupled device camera and imported into ImagePro Plus (Media Cybernetics, Silver Spring, MD). After selecting a range of pixel color values corresponding to blue-stained nuclei, a software function generated cell count data, which were separately verified by comparing to several manually counted sections.

RESULTS

Whereas the radiation sensitivity of rodent tissue is age dependent (36, 37), initial experiments were carried out to determine the age at which the apoptotic sensitivity of C57BL/6 mice represents the sensitivity of adult CNS. Three strains of mice (C57BL/6, C3H/HeJ, and 129/Sv) were irradiated at different ages with a single dose of 50 Gy, and their spinal cords were harvested 12 h after irradiation. A total of 10–18 cross sections of spinal cord per animal (representing cervical, thoracic, and lumbar regions without bias) was stained using the TUNEL method and counterstained with hematoxylin. The highest rate of apoptosis ($1.1 \pm 0.2\%$ per spinal cord section) was observed at the earliest time point tested (8 weeks of age) and gradually decreased with time, reaching a plateau at 16 weeks and beyond ($0.5 \pm 0.1\%$ per spinal cord section). Therefore, all experiments in this series were carried out with mice at 16 weeks of age.

To further characterize the apoptotic response to radiation in the CNS, time course and radiation dose-response studies were carried out. Fig. 1 depicts the dose response in spinal cord sections of duplicate mice at several time points within a 24-h period. Previous work on the radiation response of the mature rat CNS reported peak levels of apoptosis in the subependymal zone of the brain that occurred at 6–8 h after irradiation (38), and peak levels of apoptosis occurred at 10–12 h in the spinal cord (10). Our analysis of the adult mouse CNS confirmed this time course. The apoptotic response was dose dependent and peaked at 12 after irradiation (Fig. 1). Similar results could be observed in various regions of the brain, *e.g.*, hippocampus and pons (data not shown). For subsequent experiments, the dose of 50 Gy was preferred to increase the statistical significance of cell counting of low frequency events. This dose is likely to have relevance to biological phenomena because previous studies showed that single-dose radiation of less than 10 Gy produced no morphological changes in the CNS, whereas significant early or latent effects were seen with doses between 20 and 40 Gy (39). Furthermore, fractionated radiation in the range of 45–60 Gy represents the lower tolerance threshold in humans (40). Thus a 50 Gy single dose to the rodent CNS would be expected to produce sublethal, subacute effects near the lower tolerance threshold for the CNS (41).

In the experiments quoted above, the absolute numbers of apoptotic cells, rather than the percentage, were used to quantify the response to radiation. However, it should be noted that previous studies reported that whereas the numbers of neurons may vary considerably among different spinal cord levels, the total numbers of cells, including neurons, glial cells, oligodendrocytes, and endothelial cells, remained somewhat constant (42, 43). The present studies confirmed these findings. Image analysis of hematoxylin-stained spinal cord sections

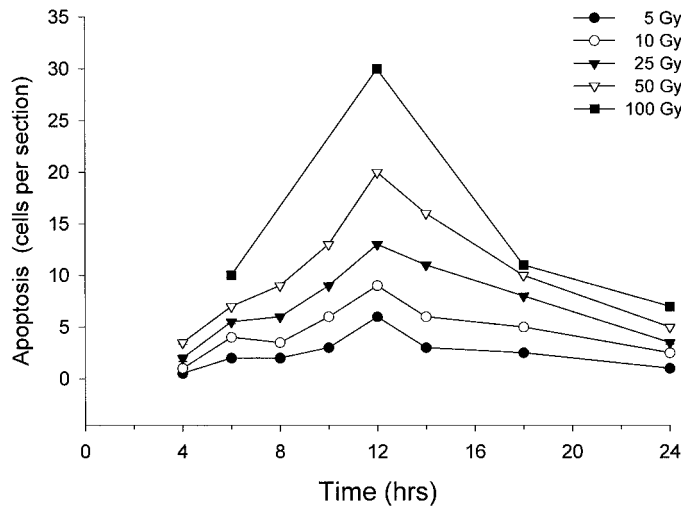


Fig. 1. Time course and dose response. Four-month-old mice were irradiated with whole body γ -radiation at various doses, and the CNS was harvested at various time points, as indicated. Paraffin-embedded cross sections of the spinal cord were stained using the TUNEL method, and the number of positively stained nuclei was counted ($n = 2$ mice, 8–12 sections/mouse). SE was $<10\%$.

of 16 week old C57/BL6 mice revealed that the total number of cells was consistent across the total length of the cord, averaging 1667 ± 318 cells per cross section. It should also be noted that no significant variations between individual mice of the same or different strains were discerned (data not shown). For example, the average cross section of 16-week-old ASM KO mice had a mean of 1600 ± 294 cells. These data indicate that in evaluating apoptotic responses to radiation in the spinal cord, it is legitimate to report the absolute number of apoptotic cells rather than a percentage of apoptotic cells per section. Furthermore, in irradiated spinal cord specimens, the total number of apoptotic cells [range, 0.7–1.4%, in agreement with the studies of Li *et al.* on rat spinal cord (10, 11)] was also found to be constant across different cord levels and across strains (see controls in Fig. 3B).

To identify which specific cell types were undergoing apoptosis, we used double staining procedures with cell phenotype-specific reagents. In this study, we describe results pertaining to endothelial cells. Widely used antibodies directed against specific adhesion molecules [*e.g.*, PECAM-1 (CD31) and E-selectin (CD62e)] are effective in specifically identifying endothelial cells in several tissues, but not in the CNS, where these cell surface markers are down-regulated coincident with the development of the blood brain barrier (34, 35). Consistent with this observation, we found that staining with an antibody against CD31 failed to stain microvessel endothelium within the brain (data not shown). In contrast, lectin staining, such as staining with LEL and RCA-1, has been shown to reliably label endothelium in the CNS (28–33, 44). The LEL staining method used in the present study is a single-step procedure and preferentially enhances endothelial staining while reducing microglial staining. Fig. 2 shows double labeling of cells with LEL and TUNEL at high magnification ($\times 1000$). An endothelial cell exhibiting intensely fluorescent LEL staining (Fig. 2A, *top*) is the same cell whose apoptotic nucleus is TUNEL positive (Fig. 2A, *middle*). These images were digitally superimposed to demonstrate the colocalization of these two markers (Fig. 2A, *bottom*). Lectin stains can also label microglia (30–33), the resident tissue macrophages of the CNS. The distinct morphology of microglia is demonstrated in Fig. 2B, whose significantly weaker staining has been enhanced in this exposure only for the purposes of reproduction for publication. The double stain studies revealed that the fraction of endothelial cells in the total population of cells under-

going apoptosis at 12 h after exposure to 50 Gy was 16–20%. The majority of apoptotic cells that were nonendothelial are likely to be glial, based on morphological criteria, in agreement with data reported by Li *et al.* (10).

To explore the mechanism of radiation-induced apoptosis in the CNS endothelium of the adult mouse, we studied the effects of i.v. injection of aFGF and bFGF. In previous studies, we demonstrated that bFGF serves as an antiapoptotic survival factor for endothelial cells irradiated *in vitro* and in a lung model *in vivo* (12, 16, 17, 45). The effect of FGF in the murine CNS was first assessed by treating animals with three equal doses of aFGF or bFGF, which were administered i.v. immediately before and after, and at 1 h after 50 Gy of irradiation (total dose delivered, 0.45–4.5 $\mu\text{g}/\text{mouse}$). TUNEL-positive apoptotic cells were counted in CNS specimens obtained 12 h after irradiation. Both bFGF and aFGF reduced the total level of apoptosis by approximately 50% (Fig. 3A). All treated animals were significantly different from sham-injected controls ($P < 0.001$). Similar significant reductions in apoptosis were measured in two strains of

A.



Endothelial cells
(LEL-TRITC)

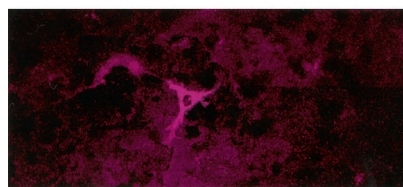


Apoptosis
(TUNEL-DAB)



Composite

B.



Microglial cell
(LEL-TRITC)

Fig. 2. A, histochemical, fluorescent, double labeling of endothelial cells undergoing apoptosis in the irradiated CNS. Magnification, $\times 1000$. *Top*, LEL conjugated to rhodamine (LEL-TRITC) brightly stains endothelial cells in paraffin sections of the CNS. Intense endothelial staining is evident at all levels of magnification. *Middle*, apoptosis in the same section is revealed by the TUNEL reaction using the brown chromogen DAB (TUNEL-DAB). *Bottom*, composite image showing specific, overlapping double staining in one endothelial cell undergoing apoptosis. The quantification of endothelial cell apoptosis is shown in Tables 1 and 3. B, microglial staining. The very different and easily recognized multipolar morphology of microglial cells is also revealed with LEL staining. However, with this method, microglial staining is very faint and is observable only at the highest magnification ($\times 1000$). This image was overexposed and contrast-adjusted for the purpose of publication.

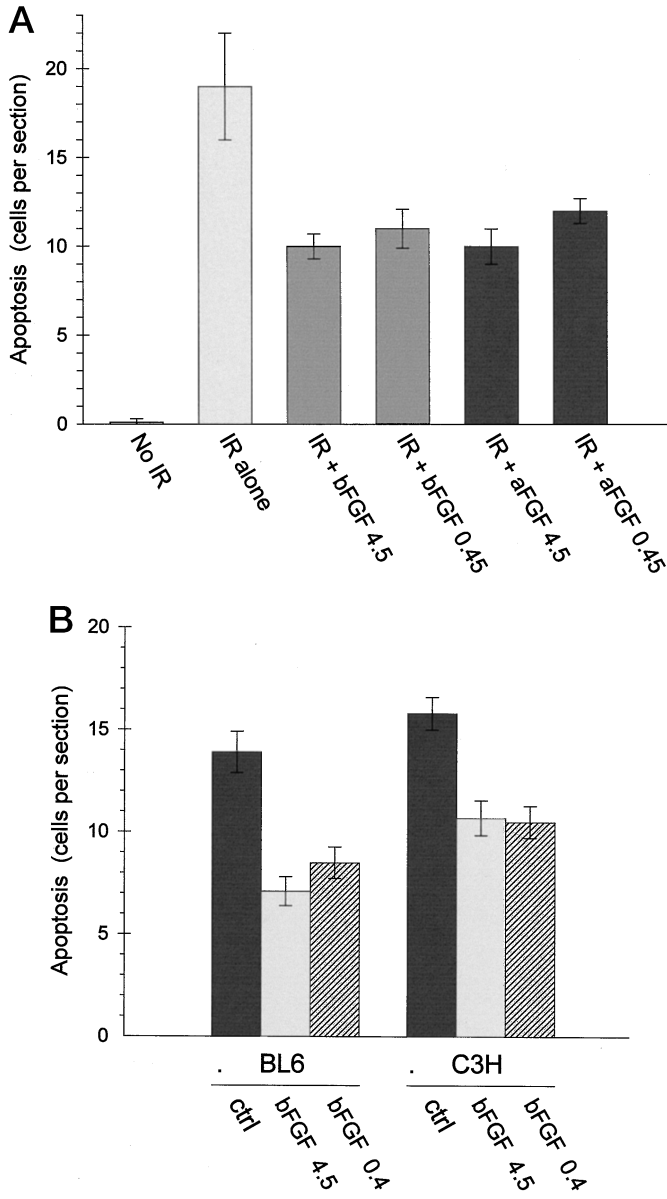


Fig. 3. A, radioprotection by FGFs. Retro-orbital i.v. injections of aFGF or bFGF reduced apoptosis assessed by TUNEL staining in the spinal cord at 12 h after irradiation with 50 Gy ($n = 2$ mice; 16–20 sections/mouse). FGFs were administered in three equivalent doses totaling 4.5 or 0.45 μg per 26–30-g mouse. [All treated animals were significantly different from sham-injected controls ($P < 0.001$).] B, FGF radioprotection and mouse strain differences. bFGF was administered via i.v. injection to 16-week-old C3H or BL6 mice, which were then irradiated with 50 Gy ($n = 2$ mice) and harvested after 12 h, and TUNEL-stained cells were counted to reveal the total number of cells undergoing apoptosis in spinal cord sections. Apoptosis in treated animals was significantly different from that in sham-injected controls ($P < 0.001$); no significant difference was seen between strains ($P = 0.08$).

mice tested, C3H/HeJ and C57BL/6 ($P < 0.001$ each; Fig. 3B). Differences between strains were not significant ($P = 0.08$). To explore whether the antiapoptotic effect of FGF was specific to the endothelial cell subpopulation of the irradiated CNS, the double labeling technique with TUNEL and LEL was used. Table 1 shows that similar to the effect of bFGF on the total cell population, treatment with bFGF resulted in an approximately 50% reduction in endothelial cell apoptosis. These ratios remained approximately the same in separate experiments with varying doses of radiation (1, 5, 10, and 20 Gy) and a constant dose of bFGF (data not shown). These data indicated that whereas FGF may protect more than one of the subpopulations of CNS cells, endothelial cells *in vivo* are indeed defi-

nately radioprotected, as has been observed previously *in vitro* and in other organs *in vivo* (12, 16, 46–50).

Previous studies of cultured endothelial cells showed that bFGF blocks radiation-induced apoptosis (17, 18, 45), likely via inhibition of ASM-mediated hydrolytic degradation of membrane sphingomyelin (14, 15). Furthermore, ASM KO mice that have a defect in ceramide generation (26) exhibit resistance to the apoptotic effects of radiation *in vivo* (14). A comparison of irradiated ASM KO mice with wild-type controls in the present studies showed that the total number of apoptotic cells was decreased 50–75% in the spinal cords of ASM KO mice (Fig. 4). Quantitative differences between wild-type and ASM KO mice were also evident in different regions of the brain, such as the hippocampus (Fig. 5), midbrain, and hindbrain (data not shown). Differences between wild-type and ASM KO mice were significant (Table 2). TUNEL/LEL double staining to identify the endothelial cell subpopulation showed a 3-fold difference between the wild-type and KO strains (Table 3). These data suggest that the effect of radiation to induce apoptosis in the cells of the CNS microvasculature is mediated via the ASM/ceramide pathway.

DISCUSSION

In the present studies, we demonstrated that radiation induces an apoptotic response in the CNS at times and dose ranges relevant to

Table 1 Apoptosis in endothelial cell subpopulation in the spinal cord of bFGF-treated mice

Spinal cord sections of mice that were irradiated and received sham or bFGF injections (4.5 $\mu\text{g}/\text{mouse}$) were harvested at 12 h ($n = 3$ mice, 16–20 sections each) and double stained with LEL-TRITC and TUNEL-DAB to specifically label apoptotic endothelial cells (see “Materials and Methods”). Double-positive cells were counted, and the means were subjected to paired *t* tests for statistical significance.

	Endothelial apoptosis per section mean \pm SE	<i>t</i> test
No irradiation	0.4 \pm 0.3	
50 Gy + sham	4.3 \pm 0.9	$P < 0.0001^a$
50 Gy + bFGF	2.0 \pm 0.6	$P < 0.001^b$

^a Comparison with unirradiated control.

^b Comparison with irradiation with sham injection.

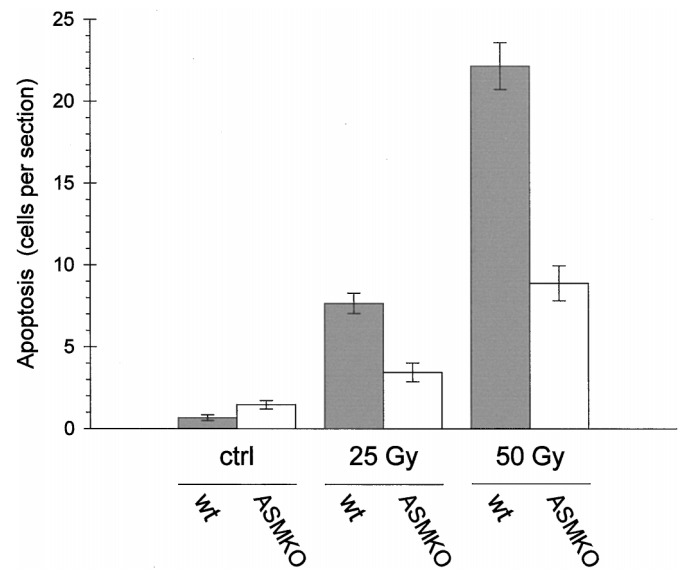


Fig. 4. Reduced apoptosis in spinal cord sections of ceramide-deficient ASM KO mice. ASM KO and wild-type mice (C57BL/6 \times SV129/J) were irradiated with 25 or 50 Gy and harvested after 12 h, and TUNEL-positive cells were counted. Apoptosis in irradiated ASM KO animals was significantly different from that in paired, irradiated controls ($P < 0.01$).

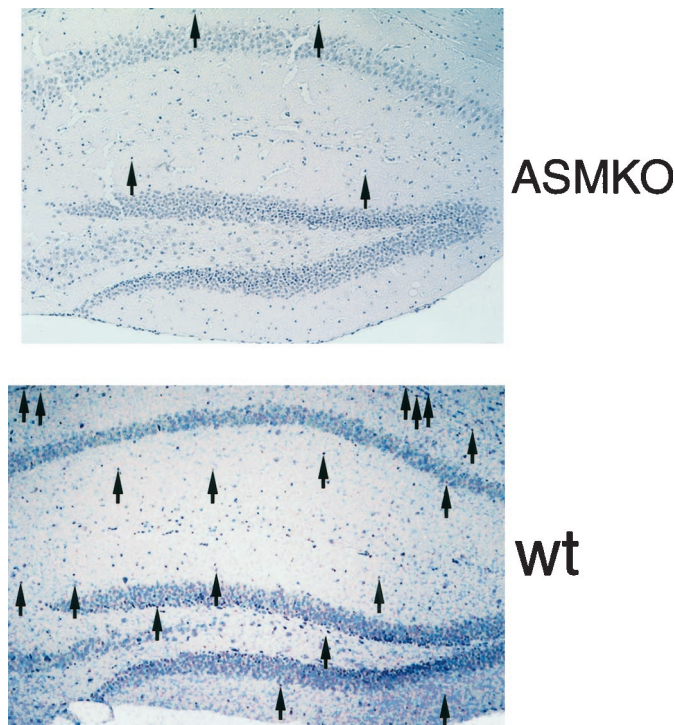


Fig. 5. Reduced apoptosis in hippocampal sections of ceramide-deficient ASM KO mice. In these panels depicting the hippocampus ($\times 100$; counterstain, hematoxylin), arrows have been placed beside TUNEL-positive nuclei that are not apparent at this low-power magnification. Identification of TUNEL-stained cells was done at $\times 400$ and $\times 1000$. See Table 2.

acute radiation toxicity. After single-dose irradiation, there was evidence of ongoing apoptosis between 4 and 24 h after exposure, which peaked at 12 h. The peak incidence of apoptosis was 0.7–1.4% of the cells in spinal cord sections. These time frames and the incidence are consistent with the observation of Li *et al.* (11), who showed in rat spinal cord that apoptosis occurred throughout the first 24 h after single-dose irradiation and peaked at 12 h at an incidence of 3%. Furthermore, that study also demonstrated that this level of ongoing apoptosis translated into an 18% loss of spinal cord cells by 24 h. This magnitude of apoptosis is likely to have functional consequences for the generation of radiation toxicity.

Our present studies also showed that 16–20% of the cells undergoing apoptosis were endothelial cells, whereas the rest involved glial subpopulations of the CNS parenchyma. It has been estimated that the number of endothelial cells in the adult mouse spinal cord is 2.50×10^6 of a total population of 13.08×10^6 cells (42), representing approximately 20% of the total. Hence, the incidence of endothelial apoptosis was proportional to the endothelial cell fraction of the total CNS cell population. Whereas the peak incidence of endothelial apoptosis appears to be low, the overall apoptotic response over the first 24-h period after radiation may be considerable and significant for the generation of tissue responses. Consistent with this notion is the study by Ljubimova *et al.* (9), which reported that 15% of the CNS endothelium is lost by 24 h after exposure to 25–100 Gy.

The fact that both endothelial cells and other parenchymal CNS cells undergo concomitant apoptosis leaves open the question of which component is critical to the evolution of acute radiation toxicity in the CNS. In previous studies, we demonstrated that microvascular endothelial apoptosis was the primary and critical response in the generation of tissue damage by radiation and other stresses. The microvascular endothelium was the earliest tissue component to undergo apoptosis in the irradiated lung of C3H/HeJ mice (12, 16, 17)

and in the small intestine, lung, and fat tissue of C57BL/6 mice during experimental septic shock (13). The critical role of this response in the evolution of tissue damage was suggested by the fact that both endothelial apoptosis and the eventual tissue damage were abrogated by i.v. bFGF therapy. Furthermore, ASM KO mice were found to be refractory to lung irradiation- and LPS-induced microvascular endothelial apoptosis, tissue damage, and animal death in response to these stresses (13, 14). The present studies showed that in the CNS, both FGF and ASM deficiency reduced radiation-induced apoptosis in the endothelial compartment. However, because endothelial apoptosis and nonendothelial apoptosis occur simultaneously, whether apoptotic damage to the microvasculature is critical to the pathogenesis of acute radiation damage to the adult mouse CNS remains unclear. The finding that bFGF and ASM deficiency reduces the apoptotic response to radiation provides a possible approach to further explore whether this acute apoptosis, over the long term, has relevance to early or late CNS injury.

Whereas the present studies provided evidence for radiation-induced endothelial apoptosis, prior investigations by Li *et al.* (10, 11) failed to detect endothelial cell apoptosis in the irradiated CNS. Differences in the histochemical assays to identify the cell types undergoing apoptosis may have accounted for this apparent discrepancy. Whereas we used the TUNEL/LEL double labeling technique to distinguish between endothelial and nonendothelial apoptosis, Li *et al.* used single-agent staining with either the Leu-7 antibody, anti-GFAP antibody, or the RCA-1 lectin (10, 11). In the Li *et al.* studies, apoptotic cells were stained only by the Leu-7 antibody, leading to the conclusion that only oligodendrocytes undergo apoptosis in response to CNS irradiation. Leu-7 labels the myelin-associated glycoprotein of oligodendrocytes and oligodendrogliomas because the carbohydrate residues of this protein contain the HNK-1 epitope (51–53). However, the HNK-1 epitope also occurs in a class of glycolipids known as sulfoglucuronosyl paraglobosides, which are present in brain microvascular endothelial cells (54–56). These sulfo-glycolipids are thought to mediate activated lymphocyte attachment to endothelial cells and subsequent infiltration into the parenchyma of the CNS. The HNK-1 epitope has also been found on neurons (57, 58) and immature astrocytes (52), in addition to the population of natural killer cells and T-lymphocytes from which it was originally described (59). Hence,

Table 2 Total apoptosis in brain regions of wild-type and ASM KO mice

Wild-type (129Sv \times C57BL/6) and ASM KO mice were irradiated with 50 Gy, and tissues were harvested at 12 h. Total number of TUNEL-positive, apoptotic cells was counted in different, matched regions of the brain ($n = 2$ mice, 8–16 sections). Paired, two-tailed *t* tests were computed to estimate statistical significance.

	WT mean \pm SE	ASM KO mean \pm SE	<i>t</i> test
Hippocampus	13.4 \pm 1.1	2.7 \pm 0.2	$P < 0.0001$
Mid-pons	8.5 \pm 1.4	2.5 \pm 0.4	$P < 0.001$
Medulla	4.8 \pm 0.6	1.9 \pm 0.6	$P < 0.003$

Table 3 Apoptosis of endothelial cell subpopulation in ceramide generation-impaired ASM KO mice

Counts of apoptotic endothelial cells in spinal cord sections of wild-type (wt) or ASM KO mice, as described above.

	Endothelial apoptosis per section mean \pm SE	<i>t</i> test
No irradiation, wt	0.0 \pm 0.0	
No irradiation, ASM KO	0.2 \pm 0.2	
50 Gy, wt	5.9 \pm 1.3	$P < 0.0001^a$
50 Gy, ASM KO	2.0 \pm 0.7	$P < 0.0001^a$ $P < 0.001^b$

^a Compared with unirradiated control.

^b Compared with wild-type strain after 50 Gy.

Leu-7/HNK-1 staining appears to lack specificity and may stain CNS endothelial cells in addition to oligodendrocytes.

The present observations are also consistent with a large body of data demonstrating survival effects for FGF on several CNS cell types *in vivo* after a variety of injuries or stresses (for review, see Refs. 60–66). Furthermore, FGF has been shown to exert radioprotective effects in several non-CNS tissue systems *in vivo*. Ding *et al.* (46–48) and Okunieff *et al.* (49, 50) have reported that in C3H mice, both bFGF and, to a lesser extent, aFGF exhibit radioprotective effects in lymphoid cells and intestinal crypt cells, and our group has previously observed protection by bFGF in the lung (12, 13, 16). Although the mechanisms involved in the radioprotective effects of FGF are not fully known, evidence suggests that PKC, which serves as the effector system mediating the radioprotective effect of bFGF in primary cultures of bovine endothelium, may act by blocking sphingomyelin hydrolysis to ceramide (15, 17). Oligodendrocytes and other glial cells (61, 62, 67, 68) express FGF receptors, and oligodendrocyte apoptosis has been linked to ceramide generation in some instances (for a review, see Ref. 69). Whether bFGF protects glial elements from radiation-induced apoptosis directly or indirectly by preserving microvessels cannot be answered by the present data. Derivatized forms of bFGF, either biotinylated or radiolabeled with ^{111}In or ^{125}I , failed to gain access to the parenchyma of the brain and remained in the intima of capillaries (16, 70), and lacked protective effects, whereas metabolically labeled [^{14}C]bFGF freely crossed the blood brain barrier and exerted protective effects (71). Further experimentation is necessary to determine whether FGF is effective in abrogating the deleterious tissue effects of radiation on the CNS and whether it is mediated via an antiapoptotic effect on oligodendrocytes, endothelial cells, or both. The study of ASM KO mice may be useful for this distinction.

ACKNOWLEDGMENTS

We thank M. Sockie Jiao and Desiree A. Ehleiter for outstanding technical support and Drs. Mark Garzotto and Adriana Haimovitz-Friedman for scientific advice.

REFERENCES

1. Vaeth, J. M., and Meyer, J. L. *Radiation Tolerance of Normal Tissues*, Vol. 23. Basel, Switzerland: Karger, 1989.
2. Emami, B., Lyman, J., Brown, A., Coia, L., Goitein, M., Munzenrider, J. E., Shank, B., Solin, L. J., and Wesson, M. Tolerance of normal tissue to therapeutic irradiation. *Int. J. Radiat. Oncol. Biol. Phys.*, *21*: 109–122, 1991.
3. Sheline, G. E., Wara, W. M., and Smith, V. Therapeutic irradiation and brain injury. *Int. J. Radiat. Oncol. Biol. Phys.*, *6*: 1215–1228, 1980.
4. Ang, K. K., and Stephens, L. C. Prevention and management of radiation myelopathy. *Oncology (Basel)*, *8*: 71–82, 1994.
5. Myers, R., Rogers, M. A., and Hornsey, S. A reappraisal of the roles of glial and vascular elements in the development of white matter necrosis in irradiated rat spinal cord. *Br. J. Cancer*, *53* (Suppl. 7): 221–223, 1986.
6. van der Kogel, A. J. Radiation-induced damage in the central nervous system: an interpretation of target cell responses. *Br. J. Cancer*, *53* (Suppl. 7): 207–217, 1986.
7. van der Kogel, A. J., Kleiboer, B. J., Verhagen, I., Morris, G. M., Hopewell, J. W., and Coderre, J. A. White matter necrosis of the spinal cord: studies on glial progenitor survival and selective vascular irradiation. In: U. Hagen, D. Harder, H. Jung, and C. Streffer (eds.), *Radiation Research 1895–1995, Congress Proceedings*, Vol. 2, pp. 769–772. Wurzburg, Germany: International Congress of Radiation Research Society, 1995.
8. Baker, D. G., and Krochak, R. J. The response of the microvascular system to radiation: a review. *Cancer Invest.*, *7*: 287–294, 1989.
9. Ljubimova, N. V., Levitman, M. K., Plotnikova, E. D., and Eidus, L. Endothelial cell population dynamics in rat brain after local irradiation. *Br. J. Radiol.*, *64*: 934–940, 1991.
10. Li, Y. Q., Guo, Y. P., Jay, V., Stewart, P. A., and Wong, C. S. Time course of radiation-induced apoptosis in the adult rat spinal cord. *Radiother. Oncol.*, *39*: 35–42, 1996.
11. Li, Y. Q., Jay, V., and Wong, C. S. Oligodendrocytes in the adult rat spinal cord undergo radiation-induced apoptosis. *Cancer Res.*, *56*: 5417–5422, 1996.
12. Fuks, Z., Alfieri, A., Haimovitz-Friedman, A., Seddon, A., and Cordon-Cardo, C. Intravenous basic fibroblast growth factor protects the lung but not mediastinal organs against radiation-induced apoptosis *in vivo*. *Cancer J. Sci. Am.*, *1*: 62–72, 1995.
13. Haimovitz-Friedman, A., Cordon-Cardo, C., Bayoumy, S., Garzotto, M., McLoughlin, M., Gallily, R., Edwards, C. K., III, Schuchman, E. H., Fuks, Z., and Kolesnick, R. Lipopolysaccharide induces disseminated endothelial apoptosis requiring ceramide generation. *J. Exp. Med.*, *186*: 1831–1841, 1997.
14. Santana, P., Peña, L. A., Haimovitz-Friedman, A., Martin, S., Green, D., McLoughlin, M., Cordon-Cardo, C., Schuchman, E. H., Fuks, Z., and Kolesnick, R. Acid sphingomyelinase-deficient human lymphoblasts and mice are defective in radiation-induced apoptosis. *Cell*, *86*: 189–199, 1996.
15. Haimovitz-Friedman, A., Kan, C. C., Ehleiter, D., Persaud, R. S., McLoughlin, M., Fuks, Z., and Kolesnick, R. N. Ionizing radiation acts on cellular membranes to generate ceramide and initiate apoptosis. *J. Exp. Med.*, *180*: 525–535, 1994.
16. Fuks, Z., Persaud, R. S., Alfieri, A., McLoughlin, M., Ehleiter, D., Schwartz, J. L., Seddon, A. P., Cordon-Cardo, C., and Haimovitz-Friedman, A. Basic fibroblast growth factor protects endothelial cells against radiation-induced programmed cell death *in vitro* and *in vivo*. *Cancer Res.*, *54*: 2582–2590, 1994.
17. Haimovitz-Friedman, A., Balaban, N., McLoughlin, M., Ehleiter, D., Michaeli, J., Vlodavsky, I., and Fuks, Z. Protein kinase C mediates basic fibroblast growth factor protection of endothelial cells against radiation-induced apoptosis. *Cancer Res.*, *54*: 2591–2597, 1994.
18. Langley, R. E., Bump, E. A., Quartuccio, S. G., Medeiros, D., and Braunjut, S. J. Radiation-induced apoptosis in microvascular endothelial cells. *Br. J. Cancer*, *75*: 666–672, 1997.
19. Quintans, J., Kilkus, J., McShan, C. L., Gottschalk, A. R., and Dawson, G. Ceramide mediates the apoptotic response of WEHI 231 cells to anti-immunoglobulin, corticosteroids and irradiation. *Biochem. Biophys. Res. Commun.*, *202*: 710–714, 1994.
20. Chmura, S. J., Nodzinski, E., Beckett, M. A., Kufe, D. W., Quintans, J., and Weichselbaum, R. R. Loss of ceramide production confers resistance to radiation-induced apoptosis. *Cancer Res.*, *57*: 1270–1275, 1997.
21. Chen, M., Quintans, J., Fuks, Z., Thompson, C., Kufe, D. W., and Weichselbaum, R. R. Suppression of Bcl-2 messenger RNA production may mediate apoptosis after ionizing radiation, tumor necrosis factor α , and ceramide. *Cancer Res.*, *55*: 991–994, 1995.
22. Kelly, M. L., Tang, Y., Rosensweig, N., Clejan, S., and Beckman, B. S. Granulocyte-macrophage colony-stimulating factor rescues TF-1 leukemia cells from ionizing radiation-induced apoptosis through a pathway mediated by protein kinase $C\alpha$. *Blood*, *92*: 416–424, 1998.
23. Bruno, A. P., Laurent, G., Averbeck, D., Demur, C., Bonnet, J., Beltaieb, A., Levade, T., and Jaffrezou, J. P. Lack of ceramide generation in TF-1 human myeloid leukemic cells resistant to ionizing radiation. *Cell Death Differ.*, *5*: 172–182, 1998.
24. Zundel, W., and Giaccia, A. Inhibition of the anti-apoptotic PI(3)K/Akt/Bad pathway by stress. *Genes Dev.*, *12*: 1941–1946, 1998.
25. Basu, S., Bayoumy, S., Zhang, Y., Lozano, J., and Kolesnick, R. BAD enables ceramide to signal apoptosis via ras and raf-1. *J. Biol. Chem.*, *273*: 30419–30426, 1998.
26. Horinouchi, K., Erlich, S., Perl, D. P., Ferlinz, K., Bisgaier, C. L., Sandhoff, K., Desnick, R. J., Stewart, C. L., and Schuchman, E. H. Acid sphingomyelinase deficient mice: a model of types A and B Niemann-Pick disease. *Nat. Genet.*, *10*: 288–293, 1995.
27. Sanders, E. J. Methods for detecting apoptotic cells in tissues. *Histol. Histopathol.*, *12*: 1169–1177, 1997.
28. Acarin, L., Vela, J. M., Gonzalez, B., and Castellano, B. Demonstration of poly-*N*-acetyl lactosamine residues in ameboid and ramified microglial cells in rat brain by tomato lectin binding. *J. Histochem. Cytochem.*, *42*: 1033–1041, 1994.
29. Fakla, I., Hever, A., Molnar, J., and Fischer, J. Tomato lectin labels the 180 kD glycoform of P-glycoprotein in rat brain capillary endothelia and mdr tumor cells. *Anticancer Res.*, *18*: 3107–3111, 1998.
30. Seitz, R. J., Deckert, M., and Wechsler, W. Vascularization of syngenic intracerebral RG2 and F98 rat transplantation tumors. A histochemical and morphometric study by use of *Ricinus communis* agglutinin I. *Acta Neuropathol.*, *76*: 599–605, 1988.
31. Wang, X. C., Kochi, N., Tani, E., Kaba, K., Matsumoto, T., and Shindo, H. Lectin histochemistry of human gliomas. *Acta Neuropathol.*, *79*: 176–182, 1989.
32. Szumanska, G. Lectin histochemistry in the rats brain in experimental postresuscitation syndrome: early and late changes. *Folia Neuropathol.*, *34*: 76–86, 1996.
33. Nico, B., Quondamatteo, F., Ribatti, D., Bertossi, M., Russo, G., Herken, R., and Roncali, L. Ultrastructural localization of lectin binding sites in the developing brain microvasculature. *Anat. Embryol.*, *197*: 305–315, 1998.
34. Williams, K. C., Zhao, R. W., Ueno, K., and Hickey, W. F. PECAM-1 (CD31) expression in the central nervous system and its role in experimental allergic encephalomyelitis in the rat. *J. Neurosci. Res.*, *45*: 747–757, 1996.
35. Lossinsky, A. S., Wisniewski, H. M., Damska, M., and Mossakowski, M. J. Ultrastructural studies of PECAM-1/CD31 expression in the developing mouse blood-brain barrier with the application of a pre-embedding technique. *Folia Neuropathol.*, *35*: 163–170, 1997.
36. Grahn, D. Acute radiation response of mice from a cross between radiosensitive and radioresistant strains. *Genetics*, *43*: 835–843, 1958.
37. Roderick, T. H. The response of twenty-seven inbred strains of mice to daily doses of whole-body X-irradiation. *Radiat. Res.*, *20*: 631–639, 1963.
38. Shinohara, C., Gobel, G. T., Lamborn, K. R., Tada, E., and Fike, J. R. Apoptosis in the subependyma of young adult rats after single and fractionated doses of X-rays. *Cancer Res.*, *57*: 2694–2702, 1997.
39. Hopewell, J. W., and Wright, E. A. The nature of latent cerebral irradiation damage and its modification by hypertension. *Br. J. Radiol.*, *43*: 161–167, 1970.
40. Schultheiss, T. E., Kun, L. E., Ang, K. K., and Stephens, L. C. Radiation response of the central nervous system. *Int. J. Radiat. Oncol. Biol. Phys.*, *31*: 1093–1112, 1995.

41. van der Kogel, A. J. Small animal models of radiation injury to the CNS. *In*: P. H. Gutin, S. A. Leibel, and G. E. Sheline (eds.), *Radiation Injury to the Nervous System*. New York: Raven Press, 1991.
42. Bjugn, R. The use of the optical disector to estimate the number of neurons, glial, and endothelial cells in the spinal cord of the mouse, with a comparative note on the rat spinal cord. *Brain Res.*, *627*: 25–33, 1993.
43. Bjugn, R., and Gundersen, H. J. Estimate of the total number of neurons and glial and endothelial cells in the rat spinal cord by means of the optical disector. *J. Comp. Neurol.*, *328*: 406–414, 1993.
44. Bankston, P. W., Porter, G. A., Milici, A. J., and Palade, G. E. Differential and specific labeling of epithelial and vascular endothelial cells of the rat lung by *Lycopersicon esculentum* and *Griffonia simplicifolia* I lectins. *Eur. J. Cell Biol.*, *54*: 187–195, 1991.
45. Haimovitz-Friedman, A., Vlodavsky, I., Chaudhuri, A., Witte, L., and Fuks, Z. Autocrine effects of fibroblast growth factor in repair of radiation damage in endothelial cells. *Cancer Res.*, *51*: 2552–2558, 1991.
46. Ding, I., Huang, K., Snyder, M. L., Cook, J., Zhang, L., Wersto, N., and Okunieff, P. Tumor growth and tumor radiosensitivity in mice given myeloprotective doses of fibroblast growth factors. *J. Natl. Cancer Inst.*, *88*: 1399–1404, 1996.
47. Ding, I., Huang, K., Wang, X., Greig, J. R., Miller, R. W., and Okunieff, P. Radioprotection of hematopoietic tissue by fibroblast growth factors in fractionated radiation experiments. *Acta Oncol.*, *36*: 337–340, 1997.
48. Ding, I., Wu, T., Matsubara, H., Magae, J., Shou, M., Cook, J., and Okunieff, P. Acidic fibroblast growth factor (FGF1) increases survival and haematopoietic recovery in total body irradiated C3H/HeNcr mice. *Cytokine*, *9*: 59–65, 1997.
49. Okunieff, P., Wu, T., Huang, K., and Ding, I. Differential radioprotection of three mouse strains by basic or acidic fibroblast growth factor. *Br. J. Cancer*, *74* (Suppl. 27): S105–S108, 1996.
50. Okunieff, P., Mester, M., Wang, J., Maddox, T., Gong, X., Tang, D., Coffee, M., and Ding, I. *In vivo* radioprotective effects of angiogenic growth factors on the small bowel of C3H mice. *Radiat. Res.*, *150*: 204–211, 1998.
51. McGarry, R. C., Helfand, S. L., Quarles, R. H., and Roder, J. C. Recognition of myelin-associated glycoprotein by the monoclonal antibody HNK-1. *Nature (Lond.)*, *306*: 376–378, 1983.
52. McGarry, R. C., Riopelle, R. J., Frail, D. E., Edwards, A. M., Braun, P. E., and Roder, J. C. The characterization and cellular distribution of a family of antigens related to myelin associated glycoprotein in the developing nervous system. *J. Neuroimmunol.*, *10*: 101–114, 1985.
53. Nakagawa, Y., Perentes, E., and Rubinstein, L. J. Immunohistochemical characterization of oligodendrogliomas: an analysis of multiple markers. *Acta Neuropathol.*, *72*: 15–22, 1986.
54. Needham, L. K., and Schnaar, R. L. The HNK-1 reactive sulfoglucuronyl glycolipids are ligands for L-selectin and P-selectin but not E-selectin. *Proc. Natl. Acad. Sci. USA*, *90*: 1359–1363, 1993.
55. Kanda, T., Yamawaki, M., Ariga, T., and Yu, R. K. Interleukin 1 β up-regulates the expression of sulfoglucuronosyl paragloboside, a ligand for L-selectin, in brain microvascular endothelial cells. *Proc. Natl. Acad. Sci. USA*, *92*: 7897–7901, 1995.
56. Yu, R. K., and Ariga, T. The role of glycosphingolipids in neurological disorders. Mechanisms of immune action. *Ann. NY Acad. Sci.*, *845*: 285–306, 1998.
57. Reifenberger, G., Mai, J. K., Krajewski, S., and Wechsler, W. Distribution of anti-Leu-7, anti-Leu-11a and anti-Leu-M1 immunoreactivity in the brain of the adult rat. *Cell Tissue Res.*, *248*: 305–313, 1987.
58. Kalcheim, C., and Gendreau, M. Brain-derived neurotrophic factor stimulates survival and neuronal differentiation in cultured avian neural crest. *Brain Res.*, *469*: 79–86, 1988.
59. Lanier, L. L., Le, A. M., Phillips, J. H., Warner, N. L., and Babcock, G. F. Subpopulations of human natural killer cells defined by expression of the Leu-7 (HNK-1) and Leu-11 (NK-15) antigens. *J. Immunol.*, *131*: 1789–1796, 1983.
60. Oomura, Y., Sasaki, K., Suzuki, K., Muto, T., Li, A. J., Ogita, Z., Hanai, K., Tooyama, I., Kimura, H., and Yanaihara, N. A new brain glucosensor and its physiological significance. *Am. J. Clin. Nutr.*, *55*: 278S–282S, 1992.
61. Eckenstein, F. P., Andersson, C., Kuzis, K., and Woodward, W. R. Distribution of acidic and basic fibroblast growth factors in the mature, injured and developing rat nervous system. *Prog. Brain Res.*, *103*: 55–64, 1994.
62. Moccetti, I., and Wrathall, J. R. Neurotrophic factors in central nervous system trauma. *J. Neurotrauma*, *12*: 853–870, 1995.
63. Grothe, C., and Wewetzer, K. Fibroblast growth factor and its implications for developing and regenerating neurons. *Int. J. Dev. Biol.*, *40*: 403–410, 1996.
64. Bikfalvi, A., Klein, S., Pintucci, G., and Rifkin, D. B. Biological roles of fibroblast growth factor-2. *Endocr. Rev.*, *18*: 26–45, 1997.
65. Cuevas, P., and Gimenez-Gallego, G. Role of fibroblast growth factors in neural trauma. *Neurol. Res.*, *19*: 254–256, 1997.
66. Cuevas, P. Therapeutic prospects for fibroblast growth factor treatment of brain ischemia. *Neurol. Res.*, *19*: 355–356, 1997.
67. Walicke, P. A. Novel neurotrophic factors, receptors, and oncogenes. *Annu. Rev. Neurosci.*, *12*: 103–126, 1989.
68. Weisenhorn, D. M., Roback, J., Young, A. N., and Wainer, B. H. Cellular aspects of trophic actions in the nervous system. *Int. Rev. Cytol.*, *189*: 177–265, 1999.
69. Mathias, S., Peña, L. A., and Kolesnick, R. N. Signal transduction of stress via ceramide. *Biochem. J.*, *335*: 465–480, 1998.
70. Fisher, M., Meadows, M. E., Do, T., Weise, J., Trubetsky, V., Charette, M., and Finklestein, S. P. Delayed treatment with intravenous basic fibroblast growth factor reduces infarct size following permanent focal cerebral ischemia in rats. *J. Cereb. Blood Flow Metab.*, *15*: 953–959, 1995.
71. Cuevas, P., Carceller, F., Munoz-Willery, I., and Gimenez-Gallego, G. Intravenous fibroblast growth factor penetrates the blood-brain barrier and protects hippocampal neurons against ischemia-reperfusion injury. *Surg. Neurol.*, *49*: 77–84, 1998.